An experimental and numerical study on CLT panels used as infill shear walls for RC buildings retrofit

An experimental and numerical study on CLT panels used as infilled shear walls for RC buildings retrofit

F. Stazi[a]*, M. Serpilli[b], G. Maracchini[a], A. Pavone[a]

[a] Department of Materials, Environmental Sciences and Urban Planning (SIMAU), Polytechnic University of Marche, via Brecce Bianche, 60131, Ancona, Italy

[b] Department of Civil and Building Engineering and Architecture (DICEA), Polytechnic University of Marche, via Brecce Bianche, 60131, Ancona, Italy

*corresponding author. *E-mail address*: f.stazi@univpm.it
E-mail addresses: f.stazi@univpm.it; m.serpilli@univpm.it; g.maracchini@univpm.it

Abstract

Cross Laminated Timber (CLT) has been gaining more and more attention in research and professional fields as a sustainable and promising construction system for mid- and high-rise structures. The need of buildings higher than those usually built with CLT has pushed the research towards the development of innovative hybrid techniques in which steel framed structures incorporate CLT shear walls. This concept may be potentially extended to existing RC framed buildings, where infilled CLT shear walls may constitute the base of an integrated seismic and energy retrofit. In order to investigate this potentiality, this paper presents a preliminary experimental and numerical study focused on the mechanical behaviour of CLT panels used as bracing system. In particular, diagonal compression tests on 3-ply panels have been carried out, also by reproducing a direct load transmission from the RC frame to the CLT infill. A comparison with the results of similar tests on CLT panels (with different number of layers and thickness) and with unstrengthened and strengthened masonry infill walls has been also provided. In addition, numerical simulations have been carried out, in order to evaluate the changes in a RC frame lateral response when CLT infills are added. The results have proved that CLT infills may be used as strengthening solution, allowing RC frame to reach higher lateral stiffness and peak load values respect to masonry infills.

Keywords

Cross laminated timber, CLT, Infill wall, Integrated solution, Seismic retrofit, RC frame, Diagonal compression test, Diagonal strut, Push-over, FEM

1 Introduction

In Europe, 40% of the existing building stock consists of multi-story reinforced concrete (RC) framed structures built when an efficient regulatory framework for the structural and energy building design was still lacking [1–5]. Today, these buildings are liable for 36% of the total energy consumption and CO2 emissions throughout their life cycle [1] and are responsible of losses in case of seismic events (especially in terms of casualties and reconstruction costs [6–8]). A structural and energy renovation process of these buildings is then strongly needed to foster an effective transition towards a more sustainable and resilient society [1,6,8].

Common structural and energy retrofit interventions are generally carried out separately and in an un-coordinated way. Integrated approaches, aimed at contemporarily solving all building deficiencies with a unique solution, are considered more sustainable and more cost-effective than common interventions [7,9–11], allowing to minimize waste production, temporary building downtime [12], on-site work embodied energy (i.e. installation times, quantity of the employed materials, labor and on-site work duration time and costs) and negative interactions between structural and energy upgrading systems [7,8].

This notwithstanding, only few integrated retrofit solutions have been developed in the research field, mainly based on a "double skin" approach. In [13], for example, a new external infilled RC frame is connected to the existing one to improve the seismic and thermal performance of existing RC buildings (Fig. 1a). In [14], a dissipative steel façade with structural and energy functions is studied (Fig. 1b). In [7], a "double-skin" with steel shear walls is applied to an existing RC structure (Fig. 1c).

Cross Laminated Timber (CLT), a sustainable solid wood-based construction material characterized by low mass, high stiffness, good seismic behaviour and good thermal properties [15], has been also considered for its use in integrated retrofit solutions [16,17]. For example, in [16] CLT panels coupled with an aerogel insulation have been used as external shear walls for the seismic retrofit of an existing RC framed structure (Fig. 1d). A similar integrated solution is proposed in [17]. However, these works are still at a first stage and more accurate investigations on the potentiality of this material for its use in integrated retrofit are still needed.

The possibility of adding CLT infills in framed structures has been recently investigated for new steel-timber hybrid structures (see e.g. [18]). However, at the authors' knowledge, there are no studies related to the possible use of infilled CLT shear walls for the seismic retrofit of existing RC buildings. For example, several works focused on the mechanical performances of CLT panels (see e.g. [19], [20] and [21]), but few papers examined the in-plane behaviour of CLT panels under a combined stress state, as may occur in infill walls (see e.g. [22] and [23]).

Our research group is developing a novel integrated retrofit solution based on the use of CLT shear walls encased as infill in existing RC framed structures (Fig. 2a). This retrofit intervention has the main purpose of increasing the overall lateral stiffness of the structure and, consequently, reducing the lateral drift values, as demanded by different structural seismic codes. An energy efficiency upgrading can be also obtained by adding an external insulation layer directly connected to the CLT panels or leaving a vented air gap (see e.g. Fig. 2b).

The aims of the present work are: (i) to preliminary investigate, through experimental and numerical studies, the elastic and post-elastic in-plane shear behavior of CLT panels when subject to a combined stress state; (ii) to evaluate the change in the lateral response of a RC frame when CLT shear walls are added. In particular, since in-plane lateral shear tests cannot be performed without involving the steel connections contribution [15], diagonal compression tests on CLT panels have been carried out. A direct load transmission from the RC frame to the CLT infill and also its confinement effect has been also reproduced by using rigid metal shoes (Fig. 3). Moreover, numerical simulations of a CLT panel subject to diagonal compression and of a reference RC frame infilled with a CLT shear wall have been performed. This campaign represents the initial stage of a wider research program on the post-elastic behaviour of CLT infills [24].

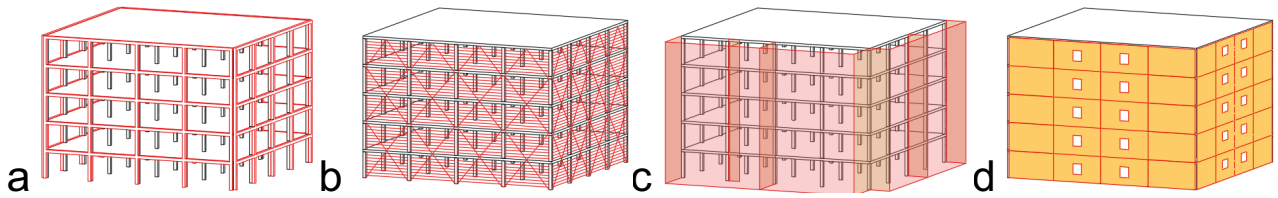

Fig. 1. a) External infilled RC frame connected to an existing RC buildings to improve the seismic and thermal performance [13]; b) dissipative steel façade with structural and energy functions [14]; c) "double-skin" with steel shear walls applied to an existing RC structure [7]; d) external CLT shear walls.

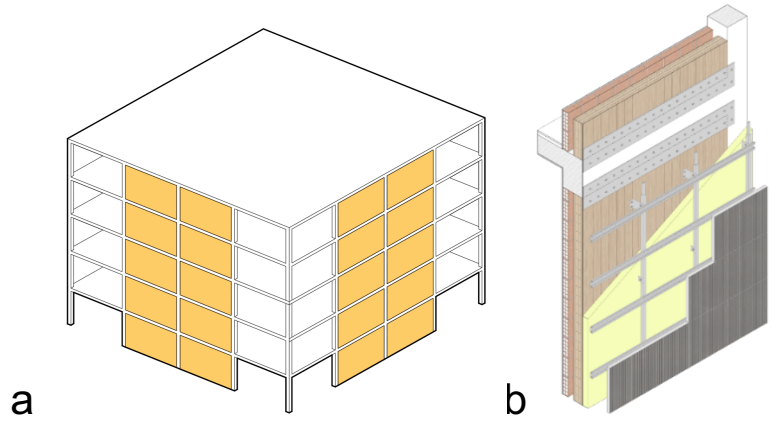

Fig. 2. a) An example of building layout with CLT infilled shear walls; b) An example of CLT infill panel with a hooked external skin (ventilated façade) for the integrated seismic and energy retrofit.

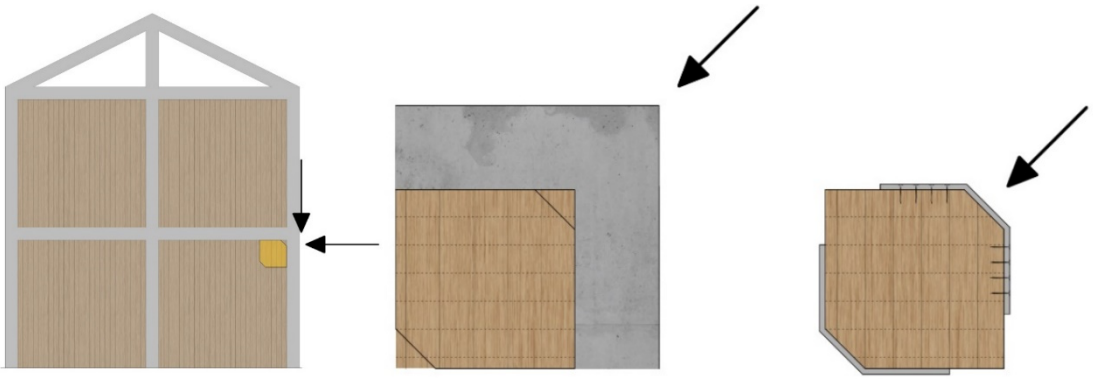

Fig. 3. Interaction between the CLT infill wall and the RC frame under seismic actions.

2 Phases, materials and methods

2.1 Phases

The present work is divided into three main phases:

- in the first phase, diagonal compression tests are carried out on CLT panels, even by adopting metal shoes to reproduce a direct load transmission from RC frame to CLT panel;
- in the second phase, a numerical simulation is carried out to identify the stress state acting in the CLT subject to diagonal compression at the end of the linear elastic phase;
- in the third phase, a numerical investigation is aimed at assessing the changes in the lateral response of a one-storey one-bay RC frame due to the insertion of a CLT infill panel.

2.2 Materials

CLT panels are solid wood elements consisting of three, five or seven stacked crosswise (typically 90 degrees) layers of softwood boards, bonded together with structural adhesive [25]. Due to their composition, these panels are able to transfer loads in all directions and are generally used as vertical load-carrying plates or horizontal slabs [26]. In this study, 3-ply CLT panels made of red spruce C24-class boards [27] and characterized by inner and outer layers thicknesses of 40 and 30 mm, respectively, have been adopted. All board faces are bonded with a polyurethane (PUR) adhesive. In Table 1, the relevant mechanical characteristics of the adopted boards have been reported, according to the manufacturer technical sheets [28].

Table 1. Mechanical characteristics of adopted red spruce C24 boards according to [28]. $E_{0,m}$ and $E_{90,m}$: mean values of the parallel-to-grain and perpendicular-to-grain moduli of elasticity; G_m: mean shear modulus; $f_{t,0,k}$ and $f_{t,90,k}$: characteristic values of the parallel-to-grain and perpendicular-to-grain tensile strength; $f_{c,0,k}$ and $f_{c,90,k}$: characteristic values of the parallel-to-grain and perpendicular-to-grain compressive strength; $f_{v,090,k}$ and $f_{v,9090,k}$: characteristic shear strength parallel-to-the-grain and perpendicular-to-the-grain (rolling shear strength) of the boards.

$E_{0,m}$ (MPa)	$E_{90,m}$ (MPa)	G_m (MPa)	$f_{t,0,k}$ (MPa)	$f_{t,90,k}$ (MPa)	$f_{c,0,k}$ (MPa)	$f_{c,90,k}$ (MPa)	$f_{v,090,k}$ (MPa)	$f_{v,9090,k}$ (MPa)
11600	*370*	*690*	*14*	*0.12*	*21*	*2.5*	*4.0*	*0.8*

2.3 Diagonal compression tests

Since reference standards for testing CLT panels under diagonal compression are lacking (see e.g. [25,26]), a testing procedure specifically developed for masonry walls [29] have been used and adapted to the specific case, even by considering the procedures adopted in similar works [22,30]. In particular, 4 CLT unconfined panels with the overall dimensions indicated in Fig. 4a, namely DC1, DC2, DC3 and DC4, have been tested with the experimental set-up shown in Fig. 4b. Then, in order to reproduce a direct load transmission from the RC frame to CLT infill, due to a hypothetical perfect bonding, and the consequent confinement effect, 2 additional panels, namely DC5 and DC6, have been tested by applying two oversized metal shoes on their upper and lower surfaces, as indicated in Fig. 4c. The perfect bonding with the RC frame, and the consequent load direct transmission, are simulated by means of connecting steel screws (see Fig. 4b).

Before testing, teflon strips have been inserted between plates and CLT panels in order to reduce the friction with the metal plates. The deformations have been measured by using 2 vertical and 2 horizontal Linear Variable Displacement Transducers (LVDT) placed on the panels lateral faces (see Fig. 4). Another LVDT has been placed on the upper face of the panel in order to measure the absolute vertical displacement. Finally, a load cell has been used to measure the applied load during tests.

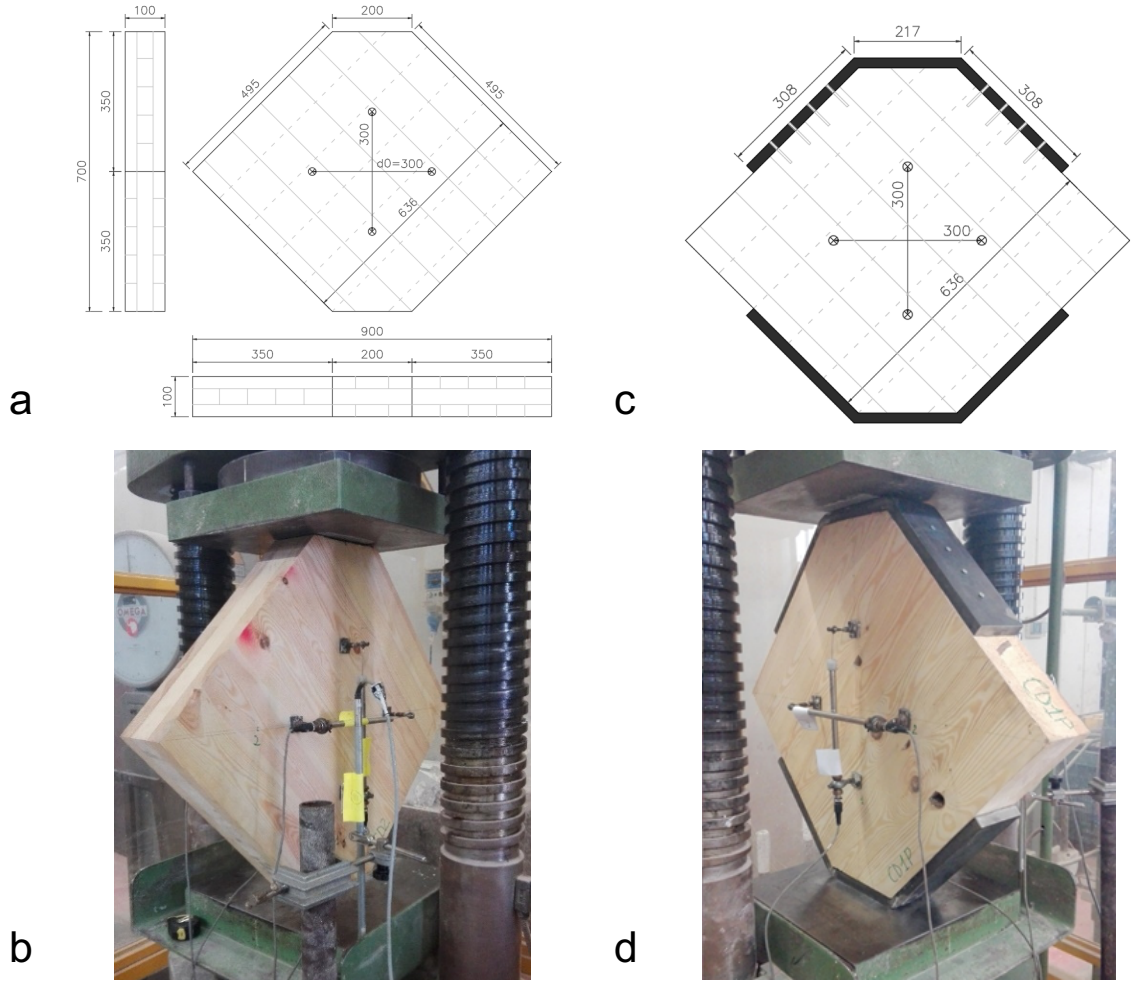

Fig. 4. a) Dimensions in millimeters of the panels used for the diagonal compression test and LVDT placement; b) dimensions in millimeters of the metal shoes used for the confined cases and LVDT placement; c) experimental set-up for the diagonal compression tests on unconfined panels; d) experimental set-up for the diagonal compression tests on confined panels.

Several analytical formulations can be used to define the internal in-plane stresses in a multi-layer material [31–34]. In this work, the analytical model proposed in [31], based on translational equilibrium equations of a representative volume sub-element (RVSE), has been adopted. Accordingly, the shear stress in the external layers τ_{xy}, the shear stress in the middle layer τ_{yx} and the internal torsional stress τ_t of a 3-ply CLT panel can be evaluated through the following equations (Fig. 5):

$$\tau_{xy} = \frac{F_{max}}{a\,(t_1+t_3)} \quad (1)$$

$$\tau_{yx} = \frac{F_{max}}{a\,t_2} \quad (2)$$

$$\tau_t = 3\,\frac{\tau_{xy} t_1}{w} \quad (3)$$

where F_{max} is the maximum load achieved during the diagonal compression test, a is the length of the panel, t_1 and t_3 the thickness of the external layers, t_2 the thickness of the internal layer and w the width of the boards.

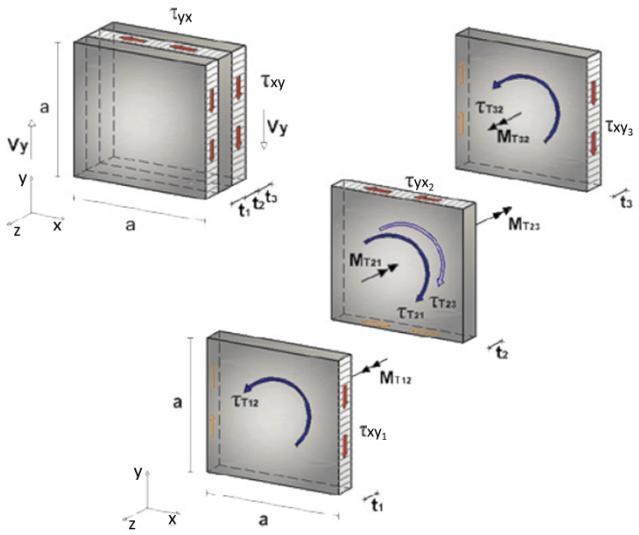

Fig. 5. Internal stress pattern in a three-layers CLT element (adapted from [22]).

Then, the mean shear stress vs shear strain curves can be obtained by referring to the core zone of the panel. This latter is defined in [35] as a square zone located at the panel center of the panel with a diagonal length equal to 0.4*a* and characterized by a high compression stresses (see Fig. 6a). Considering a linear elastic isotropic and homogeneous material, the shear strain γ in the core zone can be evaluated as [22]:

$$\gamma = \frac{2\Delta v}{d_1} \tag{4}$$

where Δv is the average variation of the core diagonal lengths measured on both side of the panel (see Fig. 6b).

Similarly, the mean shear stress inside the panel can be evaluated as:

$$\bar{\tau} = \frac{F}{\sqrt{2} \cdot A} \tag{5}$$

where F is the applied load and A is the cross-sectional area of the panel, computed as $A = t \cdot a$ being t the total thickness of the panel (i.e. $t=t_1+t_2+t_3$) and a its side length. From this relationship, the $\bar{\tau}_{max}$ can be computed as $\bar{\tau}_{max} = F_{max} / (\sqrt{2} \cdot A)$, where F_{max} is the maximum load achieved. According to [22], the value of the average shear stress in the core zone of the panel can be evaluated as:

$$\bar{\tau}_{core} = 1.429\bar{\tau} \tag{6}$$

while the maximum value of $\bar{\tau}_{core}$ can be computed as $\bar{\tau}_{core,max} = 1.429\bar{\tau}_{max}$.

Finally, the shear modulus of each CLT panel (G_{xy}) can be determined by means of a regression analysis on the linear branch of the stress-strain curve between 0.1 and 0.4F_{max} [36].

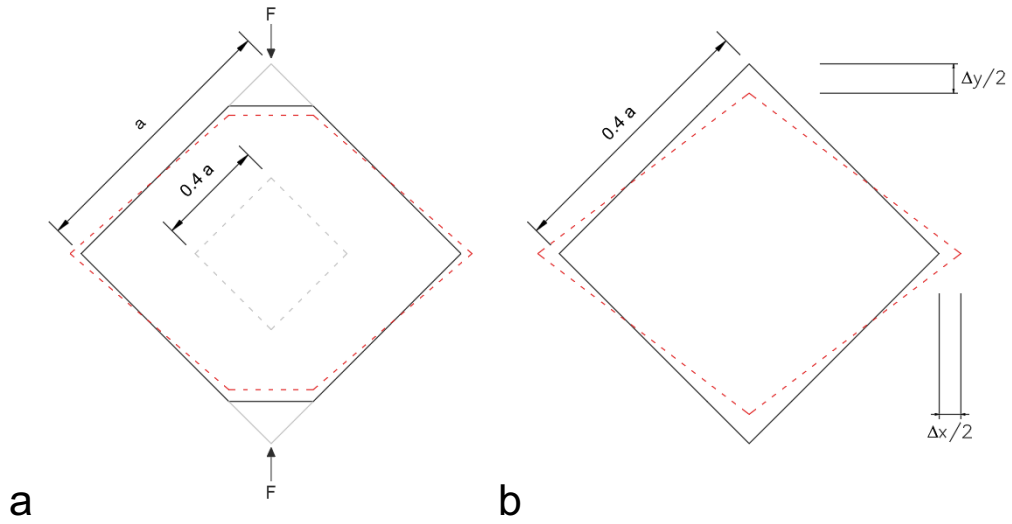

Fig. 6. a) Deformations of the panel; b) deformation of the core zone.

2.4 Numerical analyses of the diagonal compression test

In order to investigate the stress state acting in the panels during the experimental test, a numerical analysis has been carried out by using the software Midas FEA 2016 v1.1 [37]. To this aim, the CLT has been numerically modelled as a linear elastic, orthotropic and homogenized material by using 3799 eight-node quadrilateral isoparametric plane-stress elements (10x10mm). The mechanical properties of the homogenized CLT material, reported in Table 2, have been directly estimated from timber mechanical properties (Table 1) by adopting the simple homogenization approach proposed in [34], as usually made in literature (see e.g. [38,39]).

According to the experimental procedure, the panel has been assumed to be fixed at the base and an imposed vertical displacement has been applied on the upper side. In the confined case, the metal shoes have been also modeled, also assuming a perfect bonding with the CLT.

The analysis has been ended when the total reaction force obtained at the fixed base matched the experimental mean force value corresponding to the end of the linear elastic phase obtained from diagonal tests. In this way, the stress state acting on the panel just before the occurrence of first cracks have been numerically evaluated.

Table 2. Mechanical properties of the homogenized orthotropic plane stress CLT material [34]. E_x and E_y: elastic moduli parallel-to-the-grain and perpendicular-to-the-grain of the external boards, respectively; G_{xy}: shear modulus; $f_{t,x}$ and $f_{c,x}$: tensile and compressive strength parallel-to-the-grain of the external boards, respectively; $f_{t,y}$ and $f_{c,y}$: tensile and compressive strength perpendicular-to-the-grain of the external boards, respectively.

E_x (MPa)	E_y (MPa)	G_{xy} (MPa)	$f_{t,x}$ (MPa)	$f_{t,y}$ (MPa)	$f_{c,x}$ (MPa)	$f_{c,y}$ (MPa)
7108	*4862*	*690*	*8.58*	*5.87*	*12.87*	*8.8*

2.5 Numerical analysis on RC frame infilled with CLT panels

In order to investigate the change in the RC frame in-plane lateral response due to the insertions of CLT infills, a numerical study on a full scale one-storey one-bay RC frame is carried out by using the FEM software Midas FEA 2016 v1.1 [37]. A RC bare frame from literature have been adopted at this aim [40,41] (Fig. 7).

According to a meso-modelling approach (see e.g. [24] and [40]), eight-node quadrilateral isoparametric plane stress elements (50x50mm) have been used for both the RC frame and the CLT infill. The CLT infill has been modeled as an elastic orthotropic material (see Sect. 2.4); concrete and steel rebars have been modeled by adopting a smeared total strain rotating crack approach and embedded reinforcements (perfectly bonded to the surrounding finite elements), respectively. In particular, for the concrete, a parabolic behaviour in compression and an exponential law in tension have been adopted [42,43], with a crack bandwidth assumed equal to the side length of a representative quadrilateral element.

The reduction of the compressive strength due to the lateral cracking [42] and the increase of compressive strength due to the lateral confinement [44] have been also taken into account. For steel rebars, a bilinear stress-strain curve and the Von Mises criterion have been assumed in uniaxial tension. The material property values used in the analysis are reported in Table 3, estimated from available experimental data, standard prescriptions [43,45] and a model calibration (see [24] for further details). The analysis has been ended when the stress values acting in the CLT panels exceeded the strength values reported in Table 2, since these are often used in literature to check timber cracking during seismic analyses (see e.g. [38]).

Both CLT infill and RC frame have been fixed at their bases, and a perfectly bonding has been assumed at the interfaces between CLT panel and RC frame, reproducing the presence of strong connections. The same experimental loading condition adopted in [41] for the bare frame has been reproduced by using a phased analysis. In the first phase, a vertical constant load of 400kN has been applied at the top of each column and no gravity loads transmission between RC frame and CLT infill have been allowed, as in a real retrofit scenario. In the second phase, an incremental horizontal monotonic displacement has been imposed to the beam, until reaching the CLT infill stress limits.

Table 3. Material properties of concrete and steel reinforcements adopted in the modelling after calibration.

Concrete properties	*Columns*	*Beam*	*References*
Young modulus (MPa)	15000	15000	From model calibration
Poisson's ratio	0.20	0.20	CEB FIP 2010 [43]
Density (kg/m³)	2500	2500	CEB FIP 2010 [43]
Tension strength (f_{ctm}) (MPa)	2.307	2.671	Eurocode 2 [45]
Tension fracture energy (G_F^I) (N/mm)	0.0939	0.0967	CEB FIP 2010 [43]
Compression strength (f_{cm}) (MPa)	29.32	34.56	From experimental data [41]
Compression fracture energy (N/mm)	23.48	24.18	CEB FIP 2010 [43]

Steel properties	*Longitudinal*	*Transversal*	*References*
Young modulus (MPa)	210000	210000	Eurocode 2 [45]
Poisson ratio	0.30	0.30	Eurocode 3 [46]
Yield strength (MPa)	558	558	From experimental data [41]
Ultimate strength (MPa)	649	649	From experimental data [41]
Ultimate strain	0.023	0.023	Eurocode 2 [45]

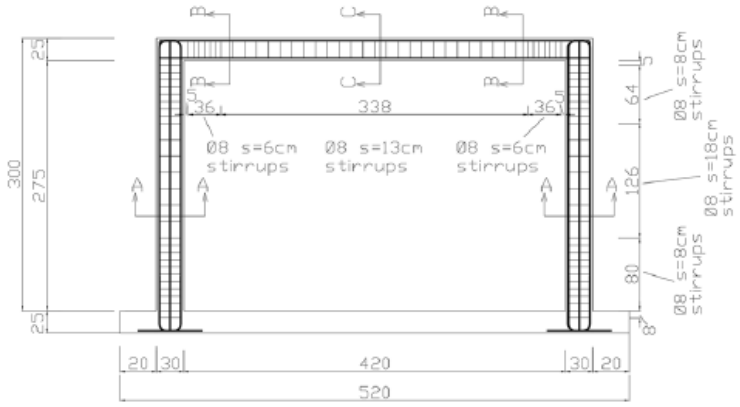

Fig. 7. Geometrical dimensions and detailing of the adopted RC bare frame (from [41]).

3 Results

3.1 Diagonal compression tests

In this section, the results of diagonal compression tests are reported. The obtained load/displacement curves and the mean core shear stress $\bar{\tau}_{core}$ vs shear strain γ curves are plotted in Fig. 8a and b, respectively, showing a similar trend for all of the tested panels. In particular, a first linear branch is obtained up to about 300 kN and 360 kN for the unconfined and confined panels, respectively, followed by a small non-linear branch up to the maximum load F_{max} (or maximum shear stress $\bar{\tau}_{core,max}$). A subsequent load drop with either a parabolic or straight shape has been then observed. In particular, a

steady state in terms of residual strength (equal to about 0.7 F_{max}) and significant deformations characterizes the post-elastic phase of the confined panels (Fig. 8a).

Concerning the damage pattern, the cracks can be related to the combination of three different failure modes [23]: pure shear, characterized by the propagation of cracks transversely to the fiber within the boards (Fig. 9a); rolling shear, characterized by cracks following the wood growth rings (Fig. 9b); boards sliding, caused by the torsional mechanisms in the interfaces due to the lack of a sufficient adhesion between boards (Fig. 9c). In particular, for the unconfined panels, at F_{max} combined mechanisms of pure shear and board sliding (torsion) have taken place, initiated at the end of the linear phase by a locally exceeded strength where the shear and tension perpendicular to the grain interacted. After reaching F_{max}, a separation in correspondence of growth rings has occurred, while only the DC2 panel has shown a failure of bond interfaces between layers (see e.g. Fig. 9d). Similar damage patterns have been observed also in the confined cases. In particular, the metal shoes have mitigated but not avoided the main damages caused by the sliding of the boards, which remains the most evident failure mode.

For each panel, Table 4 reports: the load obtained at the end of the linear phase F_l (obtained from a regression analysis); the maximum load F_{max}, the core shear stresses computed at the end of the linear branch $\bar{\tau}_{core,l}$; the computed maximum core shear stress $\bar{\tau}_{core,max}$; the perpendicular-to-the-grain mean shear stresses in the external and internal layers τ_{xy} and τ_{yx}, respectively; the mean shear stress due to torsion acting on the glued interfaces τ_t, and the shear modulus of the CLT panel G_{xy}.

As expected, the main differences between confined and unconfined panels have been obtained in terms of maximum applied loads and stiffnesses. For the unconfined panels, a mean stiffness value G_{xy} equal to 742 MPa has been obtained, which is slightly higher the expected shear stiffness value for the adopted CLT material (i.e. 690 MPa, see Table 2). For the confined ones, a higher mean value equal to 978 MPa has been obtained (with an increase of 32% respect to the unconfined ones) due to metal shoes that have varied the deformation state in the panel.

Similarly, the mean maximum forces F_{max} of the unconfined and confined panels are equal to 349 kN and 402 kN, respectively, with an average increase, passing from unconfined to confined case, of about 15%, due to the more uniform load distribution ensured by the metal shoes.

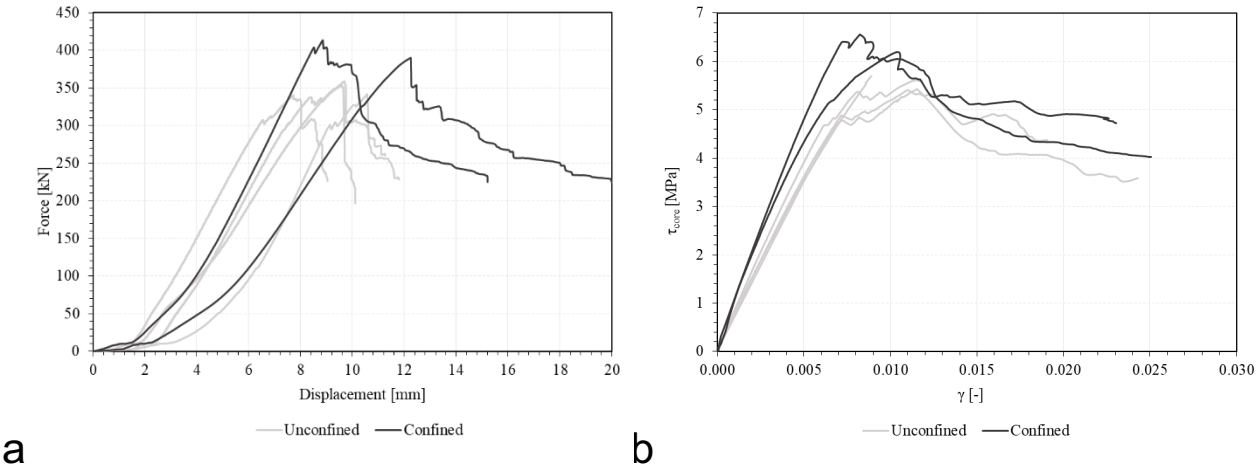

Fig. 8. a) Load/displacement curves obtained from diagonal compression tests; b) mean core shear stress $\bar{\tau}_{core}$ vs shear strain γ curves from diagonal compression tests computed according to [22].

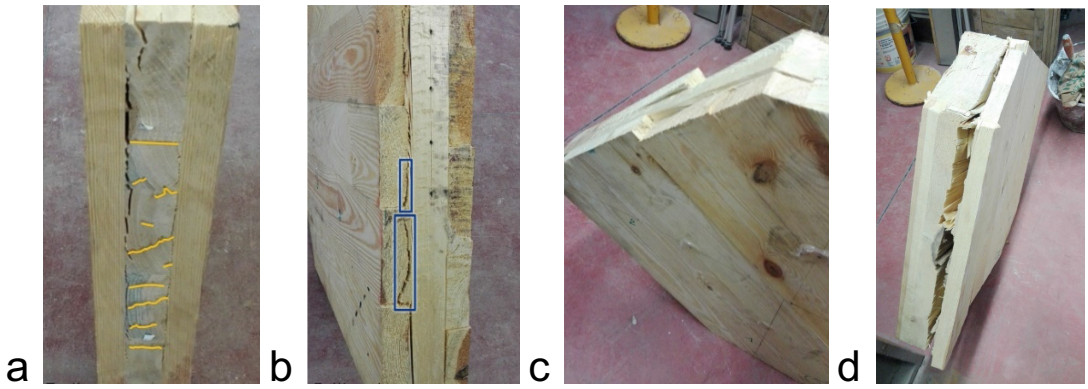

Fig. 9. Failure modes for both unconfined and confined CLT panels for a) pure shear failure mode; b) rolling shear failure mode and c) and d) boards sliding failure mode.

Table 4. Diagonal compression test results. F_l: compressive load at the end of linear branch; F_{max}: maximum compressive load; $\bar{\tau}_{core,l}$: core shear stresses computed at the end of the linear branch; $\bar{\tau}_{core,max}$: maximum core shear stress; τ_{xy} and τ_{yx}: maximum mean shear stresses perpendicular to the grain in the external and internal layers, respectively; τ_t: maximum mean shear stress due to torsion acting on the glued interfaces; G_{xy}: shear modulus of the CLT panel.

CLT panel ID	F_l (kN)	F_{max} (kN)	$\bar{\tau}_{core,l}$ (MPa)	$\bar{\tau}_{core,max}$ (MPa)	τ_{xy} (MPa)	τ_{yx} (MPa)	τ_t (MPa)	G_{xy} (MPa)
Unconfined panels								
DC1	294	353	4.67	5.61	9.25	13.88	8.33	808
DC2	359	359	5.70	5.70	9.40	14.11	8.46	717
DC3	308	341	4.89	5.41	8.93	13.39	8.03	741
DC4	293	342	4.65	5.43	8.95	13.43	8.06	702
Mean	*314*	*349*	*4.98*	*5.53*	*9.13*	*13.70*	*8.22*	*742*
Confined panels								
DC5	322	390	5.11	6.19	10.21	15.32	9.19	978
DC6	404	413	6.42	6.56	10.82	16.23	9.74	977
Mean	*363*	*402*	*5.77*	*6.36*	*10.52*	*15.78*	*9.47*	*978*

3.2 Numerical analyses of diagonal compression test

In this paragraph, the numerical results of the diagonal compression test are reported. Concerning material properties, despite the slightly difference in terms of G_{xy} values between the diagonal compression tests (742 MPa, Table 2) and the analytical calculation (690 MPa, Table 4), in the following only the results related to the experimental G_{xy} value have been reported (i.e. 742 MPa), since no significant differences have been noted in numerical results.

In Fig. 10, a comparison in terms of vertical and horizontal mean strains between experimental and numerical results is reported. As it can be seen, a good match between experimental and numerical results has been obtained for both the unconfined (Fig. 10a) and confined (Fig. 10b) cases. Due to the elastic assumption, the simulations have been ended when the total reaction force at the base of the model reached the force corresponding to the end of the linear elastic phase, i.e. at F_l (see Table 4).

The obtained maximum and minimum principal stresses at the ending step of the analysis are reported in Fig. 11. As expected, the metal shoes have modified the stress state acting in the panel, lowering the maximum values in tension and compression due to the more uniform load distribution. Anyway, in both confined and unconfined cases, the highest principal tensile stress has been reached in the center of the panel.

Since the experimental results highlighted that panel cracking was due to a combination of shear and tension stresses perpendicular-to-the-grain (see Sect. 3.1), the tangential (τ_{xy}) and normal stresses parallel and perpendicular to the grain of the external boards (σ_x and σ_y, respectively) have been deepen (Fig. 12). As it can be seen from Fig. 12c, for both the unconfined and confined cases a significant zone of the panel is characterized by high shear stress values, mostly ranging from about 4.00 to 5.00 MPa. Focusing on the stress state in the center, values of σ_x, σ_y and τ_{xy} equal to -1.31, -1.37 and -4.59 MPa for the

unconfined panel, and equal to -1.37, -1.20 and -4.46 MPa for the confined one have been obtained. These tangential stresses are very similar to the corresponding shear stresses for the unconfined panels $\bar{\tau}_{core,l}$ (see Table 4), thus confirming the reliability of the analytical model. Moreover, they are also similar to the characteristic shear strength parallel-to-the-grain of the boards ($f_{v,090,k}$, see Table 1).

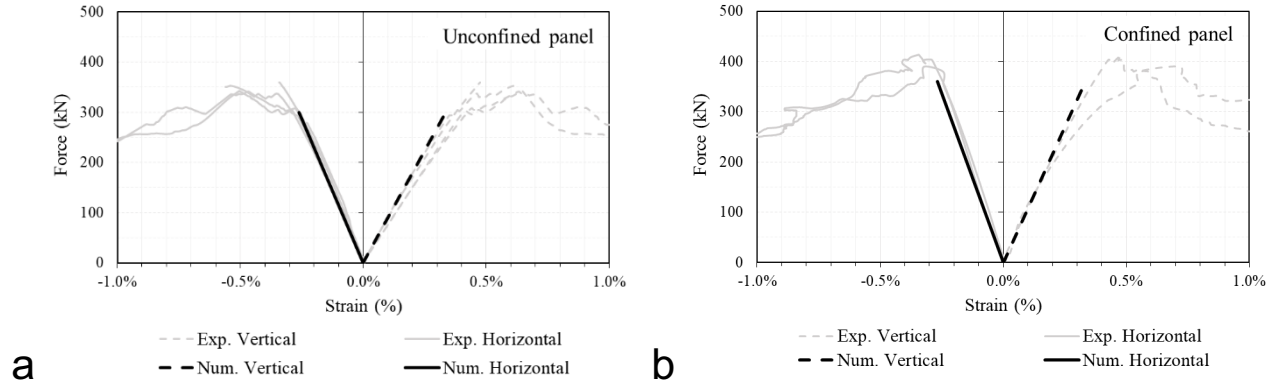

Fig. 10. Calibration results of the unconfined (a) and confined (b) CLT panels subjected to diagonal compression. Comparison between experimental and numerical results in terms of load/strain curves (mean horizontal and vertical strains measured in the LVDT gauge length).

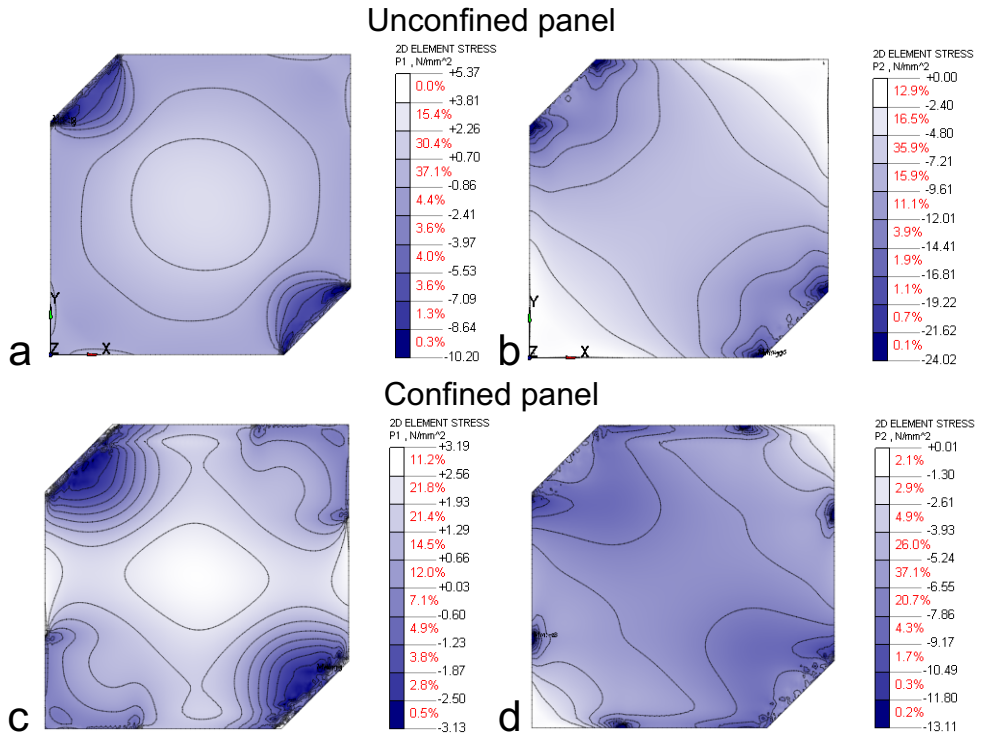

Fig. 11. Maximum (a) and minimum (b) principal stresses for the unconfined panel and maximum (c) and minimum (d) principal stresses for the confined panel at the end of the linear phase. The percentage of finite elements with stress values within the specific range is also reported.

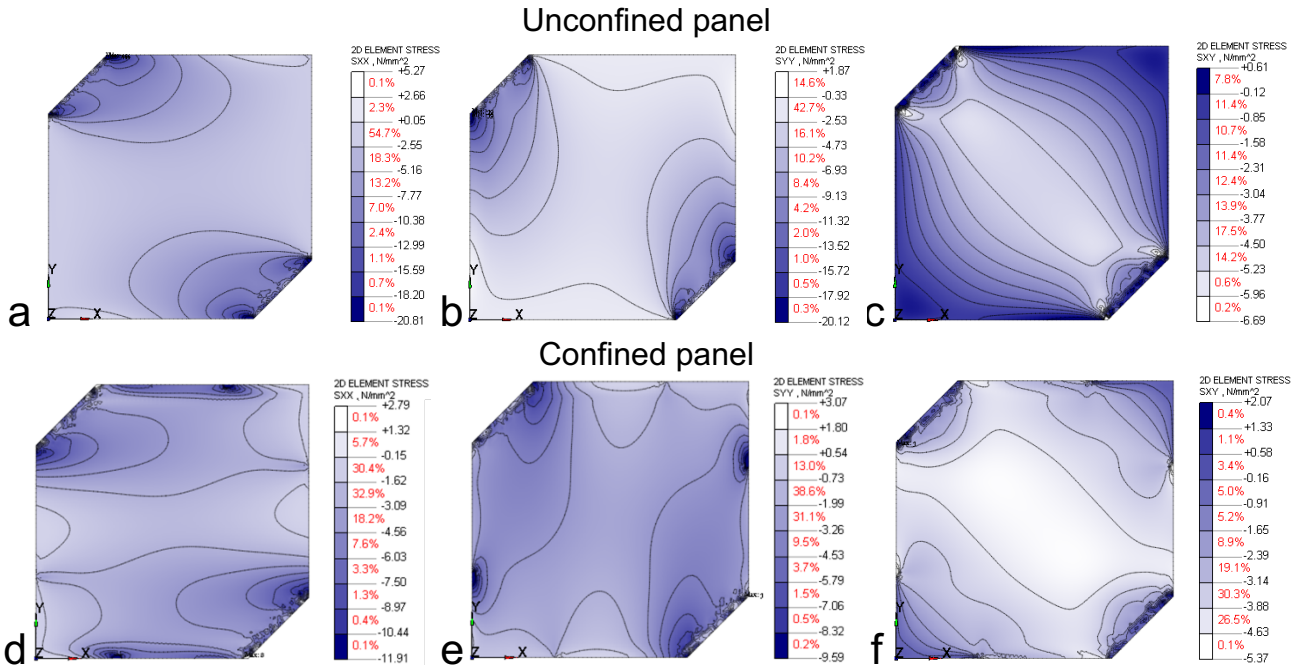

Fig. 12. Stress values at the end of the linear phase. Unconfined panel: a) normal stress values parallel to the fibers of the external boards (σ_x); b) normal stress values perpendicular to the fibers of the external boards (σ_y); c) tangential stress values (τ_{xy}). Confined panel: d) normal stress values parallel to the fibers of the external boards (σ_x); e) normal stress values perpendicular to the fibers of the external boards (σ_y); f) tangential stress values τ_{xy}. The percentage of finite elements with stress value within the specific range is also reported.

3.3 Numerical analysis on RC frame infilled with CLT panels

In this section, the numerical results on the lateral response of a RC frame infilled with a CLT panel are reported. For defining the end of the linear elastic phase of the CLT panel (and the consequent ending point of the numerical simulation), a shear strength equal to 4.00 MPa have been conservatively adopted (see Sect. 3.2), in addition to the strength parameters reported in Table 2. The corresponding drift is equal to 0.46% (13.7 mm).

The maximum and minimum principal stresses for such drift are plotted in Fig. 13a and b, denoting the formation of a diagonal compressive strut (from -3.71 to -6.00 MPa, see Fig. 13b). The values of σ_x, σ_y and τ_{xy} and the damage pattern have been also reported in Fig. 13c, d, e and f. As it can be noticed, while σ_x and σ_y are quite far from the corresponding strength values reported in Table 2 (Fig. 13c and d), τ_{xy} approaches the shear strength value in the central region of the panel (4.00 MPa). For this reason, the analysis has been stopped at this drift value. At this point, the damage pattern (Fig. 13f) shows the same damage evolution observed in the bare frame, where the first damage occurred in the columns [24].

The resulting pushover curve has been plotted in Fig. 14 and is compared with other experimental and numerical curves related to the same RC frame with different infills [40]. Although the post-elastic phase of the CLT panel has not been considered in this study, the numerical results have shown higher stiffness and peak force values for the CLT infilled RC frame if compared to both the bare and other common infilled frames. In particular, the CLT infill has allowed the RC frame reaching a global lateral stiffness of 3555 kN/m, i.e. 7 times higher than that related to the two masonry infilled RC frames (about 515 kN/m). Similarly, a maximum force equal to 1619 kN has been obtained with the CLT infill, i.e. about 4 times higher than that reached by the RC frame with the stronger masonry infill (i.e. about 440 kN with the Autoclaved Aerated Concrete masonry infill).

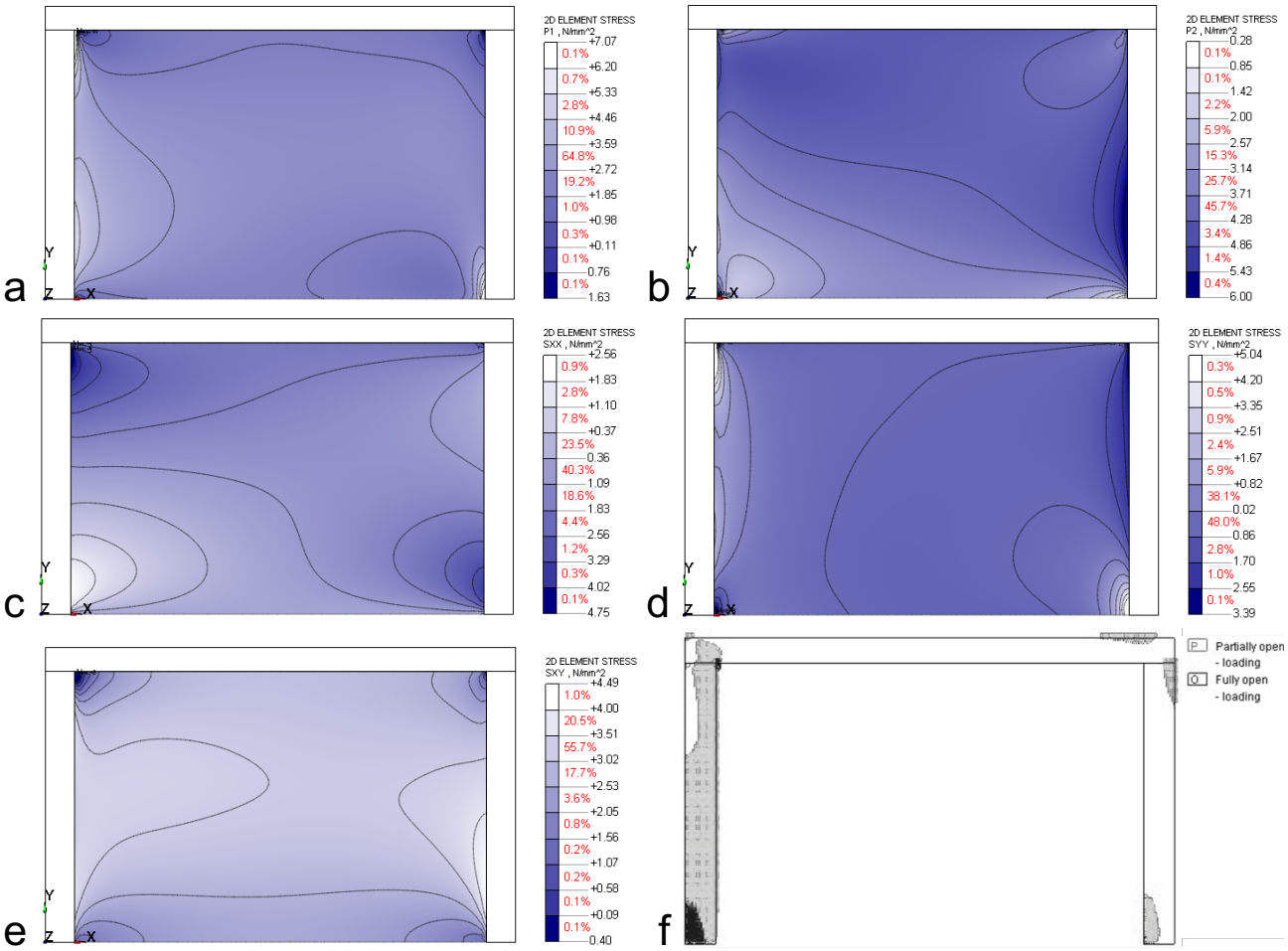

Fig. 13. Results of the numerical analysis at 0.45% drift in terms of: a) maximum principal stresses; b) minimum principal stresses; c) normal stress values parallel to the fibers of the external board (σ_x); d) normal stress values perpendicular to the fibers of the external boards (σ_y); e) tangential stress values (τ_{xy}); f) Damage pattern of the RC frame with CLT infill. Grey points: fully opened cracks; Black points: partially opened cracks.

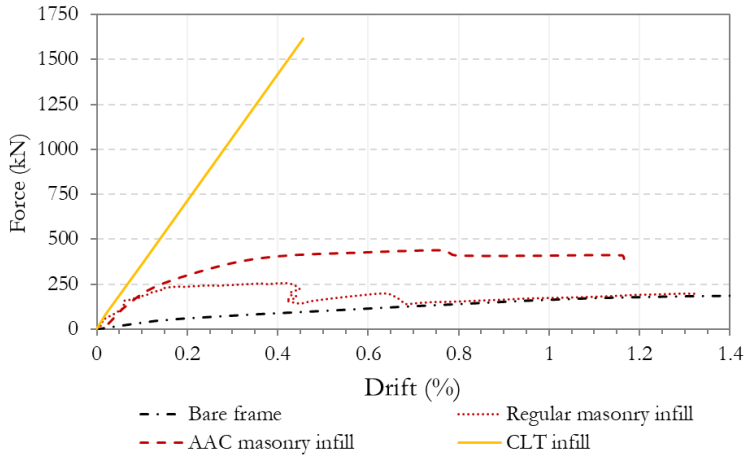

Fig. 14. Comparison between experimental and numerical pushover curves related to different infill systems. AAC: Autoclaved Aerated Concrete.

4 Discussion

The main experimental and numerical results obtained in this study are discussed and commented in this section.

The experimental campaign has allowed to investigate the post-elastic behaviour of the CLT panel in unconfined and confined condition. In particular, the load/displacement curves have shown for all the

panels a linear elastic behaviour until a first brittle drop, with maximum loads obtained for the confined case. The presence of the metal shoes, distributing the load, has reduced but not modified the damage pattern of the panels.

In Table 5, the results obtained in this study in terms of maximum load, stiffness and shear stresses are compared with the outcomes of other researches concerning the diagonal compression of unconfined CLT panels made of C24 boards (i.e. the same strength class adopted in this study) [22,30]. The 3-ply panels have shown a higher stiffness than 5-ply panels. This is likely due to the different number of preferential fracture lines, which are less in the 3-ply panels. The absence of adhesive bonding in the narrow faces of the boards (edge adhesive bonding in Table 5) for some of the 5-ply panels seems not to have affected the stiffness of the panels. Concerning the mean shear stresses in the different layers, the maximum shear stress perpendicular to the grain τ_{yx} in the internal layer at the maximum load of the unconfined panel (13.70 MPa) is comparable to the strength values reported in literature, i.e. 12.80 MPa [47]. Conversely, a higher shear stress equal to 15.78 MPa is reached for the confined panels, due to the more uniform load distribution.

Since according to the ASTM E519 [29] the $\bar{\tau}_{max}$ corresponds to the diagonal shear strength of masonry panels, in Table 6 a comparison in terms of $\bar{\tau}_{max}$ between common masonry infill panels, masonry infill panels strengthened with expanded steel plates and CLT infill panels is reported [48]. As expected, the CLT panels with metal shoe have showed the highest value, with an increase of about 25% respect to that obtained from the strengthened masonry panels (see Table 6). This is an important result even by considering that in literature the expanded steel plates have led to an increase of about 26% of the lateral strength and stiffness of an infilled RC frame [49,50].

Since the CLT panel is smaller than common infills, and that the metal shoe may have over-emphasized the confinement effect provided by a RC frame, numerical simulations of the CLT panel under diagonal compression have been carried out in order to investigate the acting stress state. At the end of the linear phase, a maximum shear stress value equal to about 4.5 MPa and spread in the center of the panel have been obtained for both the unconfined and confined case. This suggest that this value could be assumed as representative of the cracking due to shear of the adopted panel, regardless the presence and the size of eventual metal shoes. However, further studies are needed to confirm this consideration by adopting different confining tests set-up and CLT panel characteristics.

Finally, the numerical simulations on the one-bay one-story RC frame have allowed to investigate the stress state acting in the panel and the change in the lateral response of a RC frame when a CLT infilled shear wall is added and perfect bonding between CLT panel and RC frame are present. The numerical results have confirmed the experimental ones, since the CLT insertion have allowed to reach a 7 times higher global lateral stiffness and 4 times higher maximum force than that related to different types masonry infilled RC frames. In terms of displacement capacity, however, a useful comparison cannot be made due to the linear elastic assumption made for the CLT material. Anyway, these results have highlighted the high potentialities of CLT infill panels for the strengthening of infilled RC frames. However, further experimental studies are needed considering different RC frames, CLT panels and connections characteristics.

Table 5. Main dimensions of the panels and experimental shear stresses at failure. *a*: length of the CLT panel; t_{tot}: overall thickness of the CLT panel; t_1, t_2, t_3, t_4, t_5 thicknesses of the layers of the panels; F_{max}: mean maximum load for diagonal compression; τ_{xy} and τ_{yx}: mean shear stresses perpendicular to the grain in the external and internal layers, respectively; $\tau_{t,ext}$ and $\tau_{t,int}$: mean shear stresses due to torsion acting on the glued interfaces; G_{xy}: mean shear modulus of the CLT panel.

Ref.	CLT panel	a (mm)	t_{tot} (mm)	t_1 (mm)	t_2 (mm)	t_3 (mm)	t_4 (mm)	t_5 (mm)	Edge bonding	G_{xy} (MPa)	F_{max} (kN)	τ_{xy} (MPa)	τ_{yx} (MPa)	$\tau_{t,ext}$ (MPa)	$\tau_{t,int}$ (MPa)
[Present research]	3-ply	636	100	30	40	30	-	-	Yes	742	349	9.13	13.70	8.22	-
[Present research]	3-ply (Confined)	636	100	30	40	30	-	-	Yes	978	402	10.52	15.78	9.47	-
[22]	3-ply	1000	90	30	30	30	-	-	Yes	730	390	6.56	13.12	5.90	-
[22]	5-ply	1000	130	29	21	29	21	29	Yes	536	503	5.84	12.10	5.08	2.54
[22]	5-ply	1000	135	27	27	27	27	27	No	545	425	5.30	7.95	5.37	2.68
[22]	5-ply	1000	144	34	21	34	21	34	No	549	529	5.24	12.72	3.56	1.78

[30]	5-ply	640	140	40	20	20	20	40	No	549	415	6.48	16.20	5.18	1.50

Table 6. Comparison in terms of $\bar{\tau}_{max}$ between common masonry infills, masonry infills strengthened with expanded steel plates and CLT infills tested under diagonal compression.

Infill wall	Ref.	$\bar{\tau}_{max}$ (MPa)
Masonry infill (Confined)	[48]	0.66
Masonry infill strengthened with expanded steel plates (Confined)	[48]	0.62 - 3.54
3-ply CLT (Unconfined)	[Present research]	3.88
3-ply CLT (Confined)	[Present research]	4.46

5 Conclusions

This paper has presented the initial stage of a research campaign dedicated to investigate a novel strengthening method for RC framed structures in which CLT panels are used as infilled shear walls. Several monotonic diagonal compression tests have been carried out and post-elastic behaviour has been surveyed. The use of metal shoes has been also considered in order to reproduce a direct load transmission on the lateral sides of the panel. In addition, numerical simulations have been performed in order to study the stress state acting in the panel during diagonal compression tests and to investigate the change in the lateral response of a one-storey one-bay RC frame due to the insertion of a CLT infill.

From the diagonal tests, a brittle linear behaviour has been found for all the tested panels. As expected, the highest maximum load and stiffness values have been obtained for the confined panels where a residual strength of about 70% of the maximum load has been recorded. Concerning the damage pattern, the presence of the metal shoes has mitigated but not avoided the damages caused by the sliding of the boards. A comparison in terms of shear strength with strengthened masonry infill panels has been also carried out, showing that CLT infills have the highest $\bar{\tau}_{max}$, highlighting the potentiality of the CLT to strengthen a RC frame.

Numerical results on a RC frame have been then carried out to confirm this result. The CLT infill allowed RC frame reaching lower drift value and a higher peak load with respect to common masonry infills. CLT has thus high potentialities for the strengthening of RC frames. However, a more accurate investigation should be made to deepen the study of the confinement effect of the RC frame and by considering different RC frames characteristics. More advanced solution sets and innovative integrated techniques are being studied in an ongoing research. In particular, dissipative devices can be added to the system, enabling lumping damage into few sacrificial elements.

6 Aknowledgements

This work was supported by the Polytechnic University of Marche. The authors are grateful to professor Stefano Lenci who helped them during the experimental phases.

7 References

[1] A. Marini, C. Passoni, P. Riva, P. Negro, E. Romano, F. Taucer, Technology options for earthquake resistant, eco-efficient buildings in Europe: Research needs, 2014. doi:10.2788/68902.

[2] F. Clementi, E. Quagliarini, G. Maracchini, S. Lenci, Post-World War II Italian school buildings: typical and specific seismic vulnerabilities, J. Build. Eng. 4 (2015) 152–166. doi:10.1016/j.jobe.2015.09.008.

[3] G. Maracchini, F. Clementi, E. Quagliarini, S. Lenci, F. Monni, Preliminary study of the influence of different modelling choices and materials properties uncertainties on the seismic assessment of an existing RC school building, in: AIP Conf. Proc., 2017. doi:10.1063/1.4992620.

[4] E. Quagliarini, F. Clementi, G. Maracchini, F. Monni, Experimental assessment of concrete compressive strength in old existing RC buildings: A possible way to reduce the dispersion of DT results, J. Build. Eng. 8 (2016). doi:10.1016/j.jobe.2016.10.008.

[5] F. Stazi, A. Vegliò, C. Di Perna, P. Munafò, Retrofitting using a dynamic envelope to ensure thermal comfort, energy savings and low environmental impact in Mediterranean climates, Energy

Build. 54 (2012) 350–362. doi:10.1016/j.enbuild.2012.07.020.
[6] European Commission, Energy-efficient buildings PPP beyond 2013—Research and Innovation Roadmap. Document for E2B European Initiative (ECTP), 2012.
[7] A. Marini, C. Passoni, A. Belleri, F. Feroldi, M. Preti, G. Metelli, P. Riva, E. Giuriani, G. Plizzari, Combining seismic retrofit with energy refurbishment for the sustainable renovation of RC buildings: a proof of concept, Eur. J. Environ. Civ. Eng. 8189 (2017) 1–21. doi:10.1080/19648189.2017.1363665.
[8] A. Belleri, A. Marini, Does seismic risk affect the environmental impact of existing buildings?, Energy Build. 110 (2016) 149–158. doi:10.1016/j.enbuild.2015.10.048.
[9] B. Angi, Eutopia Urbanscape, in: Comb. Redev. Soc. Hous., LetteraVentidue, Siracusa, 2016.
[10] T. Dalla Mora, M. Pinamonti, L. Teso, G. Boscato, F. Peron, P. Romagnoni, Renovation of a school building: Energy retrofit and seismic upgrade in a school building in Motta Di Livenza, Sustain. 10 (2018). doi:10.3390/su10040969.
[11] F. Ascione, F. Ceroni, R.F. De Masi, F. de' Rossi, M.R. Pecce, F. de' Rossi, M.R. Pecce, Historical buildings: Multidisciplinary approach to structural/energy diagnosis and performance assessment, Appl. Energy. 185 (2017) 1517–1528. doi:10.1016/j.apenergy.2015.11.089.
[12] FEMA 398, Risk management series - Incremental Seismic Rehabilitation of Multifamily Apartment Buildings - Providing Protection to People and Buildings, (2004).
[13] V. Manfredi, A. Masi, Seismic Strengthening and Energy Efficiency: Towards an Integrated Approach for the Rehabilitation of Existing RC Buildings, Buildings. 8 (2018) 36. doi:10.3390/buildings8030036.
[14] T. Takeuchi, K. Yasuda, M. Iwata, Seismic Retrofitting Using Energy Dissipation Façades, Improv. Seism. Perform. Exist. Build. Other Struct. 41084 (2009) 1000–1009. doi:10.1061/41084(364)91.
[15] M. Izzi, D. Casagrande, S. Bezzi, D. Pasca, M. Follesa, R. Tomasi, Seismic behaviour of Cross-Laminated Timber structures : A state-of-the-art review, Eng. Struct. 170 (2018) 42–52. doi:10.1016/j.engstruct.2018.05.060.
[16] I. Sustersic, B. Dujic, Seismic strengthening of existing buildings with cross laminated timber panels, World Conf. Timber Eng. 2012 Futur. Timber Eng. WCTE 2012, July 15, 2012 - July 19, 2012. 4 (2012) 122–129.
[17] T. Dalla Mora, A. Righi, F. Peron, P. Romagnoni, Evaluation of Thermal Performance, Environmental Impact, and Cost Effectiveness of an XLam Component for Retrofitting in Existing Buildings, in: A. Sayigh (Ed.), Mediterr. Green Build. Renew. Energy, Springer International Publishing, Cham, 2017: pp. 643–655. doi:10.1007/978-3-319-30746-6_49.
[18] S. Tesfamariam, S.F. Stiemer, C. Dickof, M.A. Bezabeh, Seismic Vulnerability Assessment of Hybrid Steel-Timber Structure: Steel Moment-Resisting Frames with CLT Infill, J. Earthq. Eng. 18 (2014) 929–944. doi:10.1080/13632469.2014.916240.
[19] K.S. Sikora, D.O. Mcpolin, A.M. Harte, Effects of the thickness of cross-laminated timber (CLT) panels made from Irish Sitka spruce on mechanical performance in bending and shear, Constr. Build. Mater. 116 (2016) 141–150. doi:10.1016/j.conbuildmat.2016.04.145.
[20] I.P. Christovasilis, M. Brunetti, M. Follesa, M. Nocetti, D. Vassallo, Evaluation of the mechanical properties of cross laminated timber with elementary beam theories, Constr. Build. Mater. 122 (2016) 202–213. doi:10.1016/j.conbuildmat.2016.06.082.
[21] M. He, X. Sun, Z. Li, Bending and compressive properties of cross-laminated timber (CLT) panels made from Canadian hemlock, Constr. Build. Mater. 185 (2018) 175–183. doi:10.1016/j.conbuildmat.2018.07.072.
[22] M. Andreolli, M. Rigamonti, R. Tomasi, Diagonal Compresion Test on Cross Laminated Timber Panels, in: PROC-WCTE, 2014: p. 9.
[23] R. Brandner, P. Dietsch, J. Dröscher, M. Schulte-Wrede, H. Kreuzinger, M. Sieder, Cross laminated timber (CLT) diaphragms under shear: Test configuration, properties and design, Constr. Build. Mater. 147 (2017) 312–327. doi:10.1016/j.conbuildmat.2017.04.153.

[24] M. Serpilli, G. Maracchini, F. Stazi, Seismic solution based on the use of cross-laminated timber (CLT) panels with sliding joints as infilled earthquake bracing system for rc framed architectures, in: ReUSO 2018. L'intreccio Dei Saperi per Rispettare Passato, Interpret. Present. Salvaguardare Futur., Gangemi editore international, Roma, Italy, 2018: pp. 2251–2260.
[25] EN 16351:2015. Cross Laminated Timber - Requirements, 2015.
[26] European Organisation for Technical Approvals (EOTA), EAD 130005-00-0304. European Assessment Document on Solid Wood Slab Element To Be Used As a Structural Element in Buildings, 2015.
[27] EN 338. Structural Timber - Strength classes, 2016.
[28] OIB (Österreichisches Institut für Bautechnik), Cross Laminated Timber (CLT) Solid wood slab elements to be used as structural elements in buildings, ETA-12/0281, Vienna, 2012.
[29] ASTM E519 07. Standard test method for Diagonal Tension (Shear) in Masonry Assemblages, 2007.
[30] A. Scalbi, Nonlinear numerical approach to the analysis of Cross-Laminated Timber, 2017.
[31] M. Andreolli, R. Tomasi, A. Polastri, Experimental investigation on in-plane behaviour of cross-laminated timber elements, in: CIB-W18/45-12-4. Int. Counc. Res. Innov. Build. Constr. Work. Comm. W18 - TIMBER Struct. Meet. FORTY FIVE, 2012.
[32] M. Serpilli, S. Lenci, An overview of different asymptotic models for anisotropic three-layer plates with soft adhesive, Int. J. Solids Struct. 81 (2016) 130–140. doi:10.1016/j.ijsolstr.2015.11.020.
[33] M. Serpilli, S. Lenci, Asymptotic modelling of the linear dynamics of laminated beams, Int. J. Solids Struct. 49 (2012) 1147–1157. doi:10.1016/j.ijsolstr.2012.01.012.
[34] H.J. Blass, D.P. Fellmoser, Design of solid wood panels with cross layers, (2004) 1001–6.
[35] M.M. Frocht, Recent advances in photoelasticity and an investigation of the stress distribution in square blocks subjected to diagonal compression, in: Photoelasticity, Elsevier, 1969: pp. 25–64. doi:10.1016/B978-0-08-012998-3.50009-4.
[36] EN 408:2012. Structural timber and glue laminated timber - Determination of some physical and mechanical properties, 2012.
[37] Midas FEA, Analysis and Algorithm Manual, (2006).
[38] M.C. Porcu, C. Bosu, I. Gavrić, Non-linear dynamic analysis to assess the seismic performance of cross-laminated timber structures, J. Build. Eng. 19 (2018) 480–493. doi:10.1016/j.jobe.2018.06.008.
[39] M. Fragiacomo, B. Dujic, I. Sustersic, Elastic and ductile design of multi-storey crosslam massive wooden buildings under seismic actions, Eng. Struct. 33 (2011) 3043–3053. doi:10.1016/j.engstruct.2011.05.020.
[40] R.R. Milanesi, P. Morandi, G. Magenes, Local effects on RC frames induced by AAC masonry infills through FEM simulation of in-plane tests, Bull. Earthq. Eng. (2018). doi:10.1007/s10518-018-0353-5.
[41] G.M. Calvi, D. Bolognini, Seismic response of reinforced concrete frames infilled with weakly reinforced masonry panels, J. Earthq. Eng. 5 (2001) 153–185. doi:10.1080/13632460109350390.
[42] F.J. Vecchio, M.P. Collins, The Modified Compression Field Theory for reinforced concrete elements subjected to shear, ACI Struct. J. 83 (1986) 925–933.
[43] CEB-FIP, Model Code 2010, 2010. doi:10.1007/s13398-014-0173-7.2.
[44] R.G. Selby, F.J. Vecchio, Three-dimensional constitutive relations for reinforced concrete, Technical Report 93-02, Canada, 1993.
[45] European Committee for Standardisation (CEN), Eurocode 2 - Design of concrete structures Part 1-1: General rules and rules for buildings - EN 1992-1-1, European Committee for Standardisation (CEN), Brussels, 2004.
[46] UNI EN 1993-1-1, Eurocode 3. Design of steel structures. Part 1-1: General rules and rules for buildings, 2005.
[47] R. Jobstl, T. Bogensperger, G. Schickhofer., In-Plane Shear Strength of Cross Laminated Timber (CLT), in: CIB-W18/41-12-3, St. Andrews, Canada, 2008: pp. 1–23.
[48] A. Cumhur, A. Altundal, I. Kalkan, S. Aykac, Behaviour of brick infill walls strengthened with

expanded steel plates, Bull. Earthq. Eng. 14 (2016) 3231–3258. doi:10.1007/s10518-016-9927-2.
[49] A. Leeanansaksiri, P. Panyakapo, A. Ruangrassamee, Seismic capacity of masonry infilled RC frame strengthening with expanded metal ferrocement, Eng. Struct. 159 (2018) 110–127. doi:10.1016/j.engstruct.2017.12.034.
[50] S. Aykac, E. Ozbek, I. Kalkan, B. Aykac, Discussion on " Seismic capacity of masonry in fi lled RC frame strengthening with expanded metal ferrocement " by A . Leeanansaksiri , P . Panyakapo , A ., Eng. Struct. (2018) 0–1. doi:10.1016/j.engstruct.2018.03.014.

Highlights

- Investigation on infilled CLT shear walls for the seismic retrofit of RC frames
- Diagonal compression tests showed a high shear strength of CLT panels
- Numerical investigation on a CLT infilled RC frame were carried out
- CLT panels have high potentialities for the strengthening of infilled RC frames